

XAS and XMCD Investigation of Mn₁₂ Monolayers on Gold

Matteo Mannini,^[a] Philippe Saintavrit,^[b] Roberta Sessoli,^[a]
Christophe Cartier dit Moulin,^[c] Francesco Pineider,^[a] Marie-Anne Arrio,^[b]
Andrea Cornia,^[d] and Dante Gatteschi*^[a]

Abstract: The deposition of Mn₁₂ single molecule magnets on gold surfaces was studied for the first time using combined X-ray absorption spectroscopy (XAS) and X-ray magnetic circular dichroism (XMCD) methods at low temperature. The ability of the proposed approach to probe the electronic structure and magnetism of Mn₁₂ complexes without significant sample damage was successfully checked on bulk samples. Detailed information on the oxidation state and magnetic polarization of manganese ions in the adsorbates was

obtained from XAS and XMCD spectra, respectively. Partial reduction of metal ions to Mn^{II} was clearly observed upon deposition on Au(111) of two different Mn₁₂ derivatives bearing 16-acylthio-hexadecanoate and 4-(methylthio)benzoate ligands. The average oxidation state, as well as the relative pro-

portions of Mn^{II}, Mn^{III} and Mn^{IV} species, are strongly influenced by the deposition protocol. Furthermore, the local magnetic polarizations are significantly decreased as compared with bulk Mn₁₂ samples. The results highlight an utmost redox instability of Mn₁₂ complexes at gold surfaces, presumably accompanied by structural rearrangements, which cannot be easily revealed by standard surface analysis based on X-ray photoelectron spectroscopy and scanning tunnelling microscopy.

Keywords: magnetic properties • manganese • monolayers • X-ray diffraction • X-ray magnetic circular dichroism

Introduction

Single-molecule magnets (SMMs) have fuelled an impressive number of studies on quantum magnetism at the nano-

scale. Their unique physical behaviour^[1] can potentially be exploited to realise molecule-based devices for information storage and processing.^[2]

The magnetic addressing of individual SMMs, which is required for many of the above-mentioned applications, is now regarded as a realistic goal given the latest developments of scanning probe microscopies^[3] and nano-gap fabrication.^[4,5] Among the most promising tools for addressing the magnetism of individual molecules are spin-polarized scanning tunnelling microscopy (SP-STM)^[6] and electron spin noise STM (ESN-STM).^[7] For both techniques to be applicable, magnetic molecules need to be organised on conducting surfaces.

So far attention has mainly concentrated on the archetypal SMM, the dodecamanganese acetate cluster [Mn₁₂O₁₂(OAc)₁₆(H₂O)₄] (**1**) and its derivatives, because of their large anisotropy barrier and very-slow spin dynamics at low temperature.^[8,9] The basic structure of [Mn₁₂O₁₂(O₂CR)₁₆(H₂O)₄] complexes is sketched in Figure 1. Three main strategies of deposition have been devised to graft Mn₁₂-type complexes on gold substrates:^[10] direct deposition of suitably-functionalised molecules on native metal surfaces,^[11–13] deposition of native clusters on pre-functionalised metals,^[13–15] and pre-functionalization of both partners with

[a] Dr. M. Mannini, Prof. R. Sessoli, F. Pineider, Prof. D. Gatteschi
La.M.M., Department of Chemistry and INSTM Research Unit
Università di Firenze
Via della Lastruccia 3, 50019, Sesto Fiorentino (FI) (Italy)
Fax: (+39)0554573372
E-mail: dante.gatteschi@unifi.it

[b] Dr. Ph. Saintavrit, Dr. M.-A. Arrio
Institut de Minéralogie et de Physique des Milieux Condensés,
UMR7590
Université Pierre et Marie Curie
Case 115, 4, place Jussieu, 75252 Paris cedex 05 (France)

[c] Dr. Ch. Cartier dit Moulin
Laboratoire de Chimie Inorganique et Matériaux Moléculaires
Université Pierre et Marie Curie
Case 42, 4, place Jussieu, 75252 Paris cedex 05 (France)

[d] Prof. A. Cornia
Department of Chemistry and INSTM Research Unit
Università di Modena e Reggio Emilia
Via G. Campi 183, 41100 Modena (Italy)

Supporting information for this article is available on the WWW
under <http://dx.doi.org/10.1002/chem.200800693>.

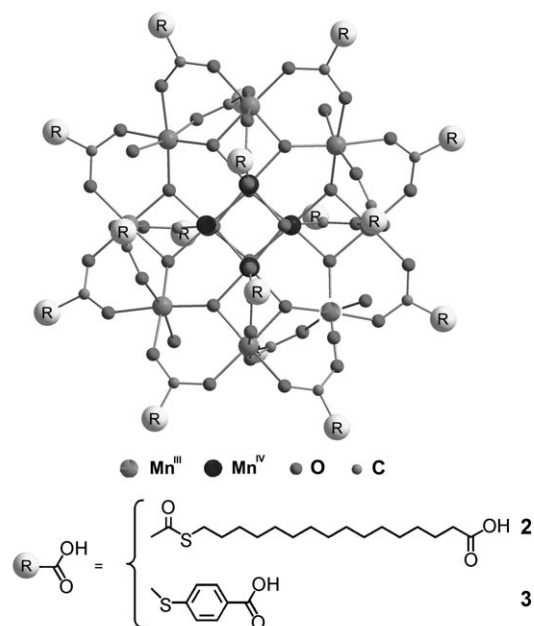


Figure 1. Molecular structure of the Mn_{12} derivatives studied in this work.

complementary groups.^[16] A crucial point is to demonstrate that SMMs remain intact on the surface. Molecular size and bidimensional arrangement are often estimated by STM.^[11–15] The chemical composition of the adsorbates can be obtained by X-ray photoelectron spectroscopy (XPS),^[11,12] although an unambiguous determination of manganese oxidation states is difficult using this technique alone.^[13] Other approaches to gain information on the electronic structure of the adsorbates have been suggested, including scanning tunnelling spectroscopy (STS)^[14] and resonant photoelectron spectroscopy (RPES).^[13,17] However the key property to be measured is the magnetisation, which in the case of (sub)monolayers of SMMs is not accessible to standard magnetometry and therefore requires other techniques to be employed for deposition.

We wish to show here that low temperature (including also the sub-Kelvin range) X-ray magnetic circular dichroism (XMCD), is sensitive enough to read the magnetism of single layers. Combined with X-ray absorption spectroscopy (XAS), it provides a unique tool to investigate the electronic structure of magnetic molecular clusters at surfaces. XMCD exploits the different absorption of X-ray photons of different helicities to gain insight into the local magnetic moment. The technique retains the chemical specificity and sensitivity of XAS, and has been used to study the magnetism of atoms and molecules on surfaces.^[18,19] Two reports on the XAS of Mn_{12} complexes at surfaces have appeared in the recent literature,^[13,17] but XMCD studies have never been carried out on Mn_{12} adsorbates. In particular we show that a semi-quantitative treatment of XAS and XMCD data provides evidence of a significant modification of the electronic and magnetic structure of the clusters that occurs during the grafting on the surface and depends on the procedure employed.

Results and Discussion

Two sulphur derivatives of **1**, especially designed to be grafted on gold, have been studied in this work, both as powder samples and as adsorbates on Au(111) surfaces: **2** ($\text{RCO}_2\text{H} = 16$ -acetylthio-hexadecanoic acid) and **3** ($\text{RCO}_2\text{H} = 4$ -(methylthio)benzoic acid) as explained in Figure 1. In the bulk phase, the XAS and XMCD spectra of **2** and **3** at Mn $L_{2,3}$ edges ($2p \rightarrow 3d$ transitions) are very similar to those reported for microcrystalline **1** (see Figure 2)^[20,21] and are consistent with the presence of anti-ferromagnetically-coupled Mn^{III} and Mn^{IV} centres.

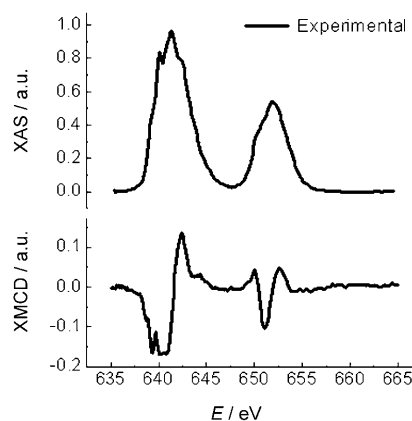


Figure 2. Normalised XAS spectrum (top) and XMCD component (bottom) at Mn $L_{2,3}$ edges recorded on a bulk sample of **3**.

The lack of a Mn^{II} signal over the entire irradiation time (up to 24 h) suggests that the set-up has been successfully optimised so as to minimise any sample damage by photo-reduction in Mn_{12} clusters. However, great care was taken to ascertain the ability of XAS and XMCD to detect subtle changes in the electronic structure of the clusters, such as a one-electron reduction. To this aim, we have also investigated a monoanionic Mn_{12} derivative (PPh_4) $[\text{Mn}_{12}\text{O}_{12}(\text{O}_2\text{CPh})_{16}(\text{H}_2\text{O})_4]$ (**4**) in the bulk phase.^[22] The extra electron is localised on a former Mn^{III} site and this complex can therefore be formulated as $\text{Mn}^{\text{II}}\text{Mn}^{\text{III}}_7\text{Mn}^{\text{IV}}_4$. The XAS and XMCD spectra of a microcrystalline sample look quite similar to those of “neutral” Mn_{12} , with a small enhancement of the dichroic signal around 639 eV, consistent with the presence of a Mn^{II} component (Figure 3).

To get more quantitative information, the experimental energy dependence of XAS spectrum intensity, $I(E)$, can be reproduced through a linear combination of model spectra $I^\alpha(E)$ obtained on suitable reference compounds containing the Mn ion in the three oxidation states ($\alpha = \text{II, III, IV}$) and in similar chemical environments [Eq. (1)]:

$$I(E) = \sum_{\alpha} c^{\alpha} I^{\alpha}(E) \quad (1)$$

From the c^{α} parameters the percentages of different valence states can be extracted as $(\%)^{\alpha} = 100 c^{\alpha} / (\sum_i c^i)$. As de-

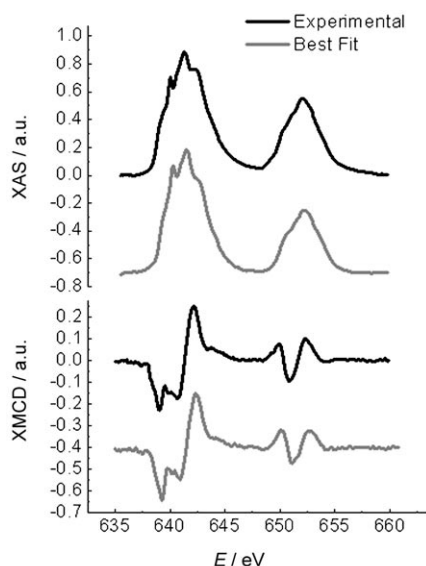


Figure 3. Normalised XAS spectrum (top) and XMCD component (bottom) at Mn L_{2,3} edges recorded on a bulk sample of **4**, the one-electron reduced Mn₁₂ derivative: the isotropic and the dichroic spectra obtained from the experimental data (black lines) are compared to the calculated ones (grey lines).

tailed in the Supporting Information, previously recorded spectra have been used to model the contributions of Mn^{II}[23] and Mn^{IV}.^[21] For Mn^{III} we checked two different procedures: i) using a standard Mn^{III} spectrum;^[21] ii) extracting a model Mn^{III} spectrum from the experimental data of **3** in the bulk phase. Very similar percentages were obtained in the two cases (see the Supporting Information). However, as far as small features in the L₃ edge are concerned, the simulation is significantly better using the latter approach. This semi-quantitative analysis of XAS data of **4** provided a Mn^{II}:Mn^{III}:Mn^{IV} ratio (5:60:35) that is in complete agreement with the expected one (8:58:33, see Table 1), thus confirming that a one-electron reduction can be clearly detected in our experimental setup.

An analogous approach can be employed to extract from the XMCD spectra semi-quantitative information on the orientation of the magnetic moments in each oxidation state. The energy dependence of the dichroic signal, $S(E)$, is expressed as a linear combination of model spectra, $S^\alpha(E)$, at the same field and temperature values [Eq. (2)]:

$$S(E) = \sum_{\alpha} c^{\alpha} \delta^{\alpha} S^{\alpha}(E) \quad (2)$$

In which α runs over the oxidation states, c^{α} are the coefficients resulting from the deconvolution of XAS spectra, and δ^{α} accounts for the average polarization of the local magnetic moment in the ap-

Table 1. Summary of XAS and XMCD results. Reported percentages are extracted from XAS spectra, whereas the arrows indicate the average polarization of each component deduced from XMCD spectra. The black arrows (pointing up) correspond to a polarization parallel to the applied magnetic field, and light grey arrows (pointing down) to the antiparallel case. The length of the arrows provides the approximate polarization intensity [δ in Eq. (2)]. The unit polarization ($\delta = \pm 1$) corresponds to the length of the arrows for **3** in the bulk phase. See also the Table in Supporting Information.

Sample	Oxidation state		
	Mn ^{II} [%]	Mn ^{III} [%]	Mn ^{IV} [%]
3 bulk ^[a]	n.d.	67	33
4 bulk ^[b]	5	60	35
2 monolayer from THF	20	65	15
3 submonolayer from THF	20	40	40
3 monolayer from CH ₂ Cl ₂	30	50	20

[a] Oxidation states percentages and polarizations for **3** bulk are imposed as demonstrated in Ref. [21]. [b] The expected Mn^{II}:Mn^{III}:Mn^{IV} ratio in **4** is 8:58:33.

plied field (positive if parallel to the field). This analysis of the XMCD data provided the following values for the polarization: $\delta^{\text{II}} = +3$, $\delta^{\text{III}} = +1$ and $\delta^{\text{IV}} = -1$. These values are very rough estimates (in particular for δ^{II} , owing to a very small c^{II} value), but their sign is in agreement with the spin structure of **4** suggested by the large spin of the ground state.^[22]

The surface sensitivity of XAS/XMCD, combined with the method of analysis developed above, allowed us to explore the nature of the molecular adsorbates. Deposition of a monolayer of **2** on Au(111) was carried out from a THF solution as previously described.^[11] An excellent agreement was found between XPS data and the expected composition, but the oxidation states of the metals could not be reliably determined. STM studies provide evidence of the presence of a homogeneous layer of objects with size comparable to the estimated molecular size^[11] as shown in Figure 4a.

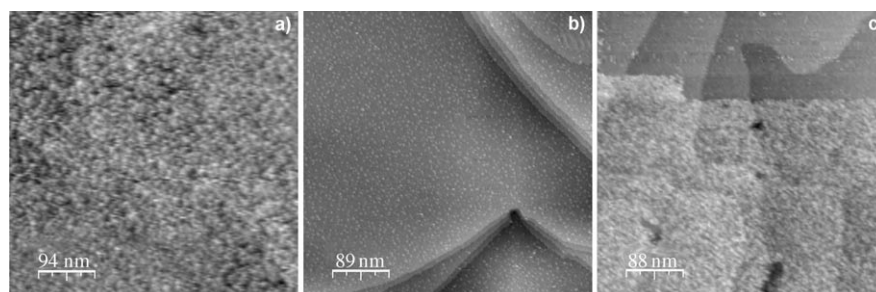


Figure 4. STM characterisation of the three different deposits of Mn₁₂ derivatives studied in this paper. a) homogeneous full monolayer of **2** deposited from THF; b) submonolayer of **3** deposited from THF; c) homogeneous full monolayer of **3** deposited from CH₂Cl₂. The upper part of image c) had been previously scanned at low bias voltage, so as to remove the monolayer

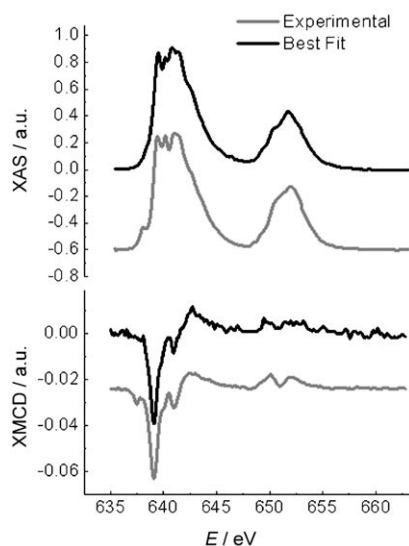


Figure 5. Normalised XAS spectrum (top) and XMCD component (bottom) at Mn $L_{2,3}$ edges recorded on a monolayer sample of **2** deposited from THF: the isotropic and the dichroic spectra obtained from the experimental data (black lines) are compared to the calculated ones (grey lines).

The XAS spectra (Figure 5) of this deposit have some similarities to those of bulk Mn_{12} derivatives, though a significant fraction of Mn^{II} is detectable. A fit of the observed intensities by using the method described above provides a 20:65:15 ratio between Mn^{II} , Mn^{III} and Mn^{IV} contributions (see the Supporting Information). This suggests a significant modification of the electronic structure, with an alteration of the average oxidation state from +3.33 in neutral Mn_{12} to +2.95. Comparison with the data obtained on **4** clearly indicates that the process cannot be described as a one electron reduction. Furthermore, comparison with the bulk composition (0:67:33) suggests that the reduction involves mainly the Mn^{IV} sites, in contrast with the established redox behaviour of bulk Mn_{12} complexes.^[24]

XAS spectra have been obtained also for adsorbates of **3** prepared from THF solution (Figure 6). This derivative, which is characterised by a much shorter and conjugated linker between the grafting group and the metal core, affords a submonolayer deposit as evidenced by STM studies (Figure 4b).^[12]

In this case, our semi-quantitative analysis provided a 20:40:40 ratio of oxidation states (av. +3.20). Even if the percentage of Mn^{II} is substantially the same as in **2**, the reduction now occurs at the expenses of Mn^{III} . The higher Mn^{IV}/Mn^{III} ratio in **3** as compared with **2** is clearly reflected in the greater extension of the L_3 edge on the high-energy side. We argue that reduction of the Mn_{12} core upon direct deposition on gold substrates from THF solution occurs irrespective of the particular ligand used to promote the grafting. In particular, according to the average oxidation states evaluated for **2** and **3**, the long alkyl spacer of **2** does not provide any shielding effect. We notice that a XAS spectrum similar to that reported in Figure 6 and quite distinct from

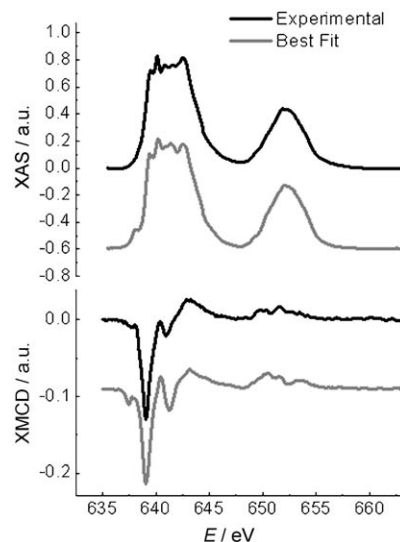


Figure 6. Normalised XAS spectrum (top) and XMCD component (bottom) at Mn $L_{2,3}$ edges recorded on a submonolayer sample of **3** deposited from THF: the isotropic and the dichroic spectra obtained from the experimental data (black lines) are compared to the calculated ones (grey lines).

that of bulk Mn_{12} was obtained by Voss et al. for another Mn_{12} derivative ($R=Ph-Ph$) deposited on Au(111) using a completely different procedure, that is, ligand exchange on a preformed monolayer of 4-mercapto-2,3,5,6-tetrafluorobenzoic acid.^[13] Although a quantitative data analysis was not attempted by those authors, this similarity suggests that core reduction cannot be considered a specific consequence of the adopted herein direct deposition procedure.

Recently^[12b] we investigated in detail the role played by different experimental parameters in the deposition of **3** on gold surfaces. In particular we found that by replacing THF with CH_2Cl_2 a full monolayer is obtained instead of a submonolayer, as shown also in Figure 4b,c. According to STM experiments, the interaction of the adsorbates with the gold surface is also significantly reduced by using CH_2Cl_2 as solvent. In fact, by operating in constant current mode and decreasing the bias voltage of the tunnelling junction (and thus approaching to the surface) the layer of clusters deposited from CH_2Cl_2 could be swept away by the STM tip. A similar weak interaction with the surface was found in monolayers of **2** deposited from THF.

The XAS and XMCD spectra of monolayer deposits of **3** obtained from CH_2Cl_2 are shown in Figure 7. The analysis of the XAS spectrum provided $Mn^{II}:Mn^{III}:Mn^{IV}=30:50:20$ with an average oxidation state of +2.90. The significant reduction of the Mn^{IV} contribution bears strong resemblance with the results obtained for monolayers of **2** deposited from THF. The type of transformation that Mn_{12} clusters undergo upon grafting on gold seems therefore to parallel the strength of interaction with the surface evidenced by STM experiments (Figure 4).

To get a deeper insight into this complex phenomenon we have also analyzed the dichroic spectra for the three mono-

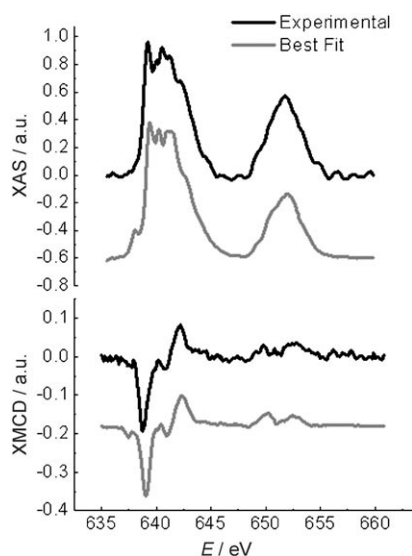


Figure 7. Normalised XAS spectrum (top) and XMCD component (bottom) at Mn $L_{2,3}$ edges recorded on a monolayer of sample of **3** deposited from CH_2Cl_2 : the isotropic and the dichroic spectra obtained from the experimental data (black lines) are compared to the calculated ones (grey lines).

layer preparation, using the method previously described. The results of the XAS and XMCD analysis are summarised in Table 1 where the length and direction of the arrows represent the polarization coefficients δ we have previously introduced. These values are only indicative but allow us to extract some additional information compared to XAS only. First of all, an apparent reduction of magnetic polarization is observed when monolayers of **2** and **3** are deposited from THF. In the temperature and field conditions of the experiments full fragmentation of the clusters to give isolated paramagnetic ions would afford full polarization $\delta^{\text{II}} = \delta^{\text{III}} = \delta^{\text{IV}} = +1$ and can consequently be ruled out. This limiting case of a complete degradation to isolated ions has been simulated and found to show a much poorer agreement with experimental spectra (see the Supporting Information). Moreover Mn^{II} ions feature a small magnetic polarization and are presumably part of exchange-coupled species. It is also interesting to point out the disappearance of the negative polarization for Mn^{IV} , which can be regarded as a fingerprint of the Mn_{12} core.

The differences observed for the monolayer of **3** prepared from CH_2Cl_2 are intriguing: in this case, larger polarizations are detected and the magnetic moment residing on Mn^{IV} ions is antiparallel to the applied field. This result cannot be attributed to the lower temperature employed for this last experiment (see the Experimental Section). The observed behaviour is therefore reminiscent of the spin structure of Mn_{12} clusters, although with a significant fraction (30%) of Mn^{II} ions.

We have therefore decided to focus our efforts and beamtime to further investigate the low temperature magnetic behaviour of this particular monolayer, in which the presence of intact Mn_{12} complexes cannot be completely ruled out.

The XCMD signal at 641 eV was recorded as a function of applied field, as at 641 eV the XMCD amplitude of Mn_{12} clusters is maximum. By sweeping the field between ± 5 T, no hysteresis was observed down to the lowest temperature reached in our experiment ($T \approx 500$ mK). The failure to detect a hysteresis loop shows that, in the most favourable scenario, the magnetic properties of Mn_{12} complexes are strongly influenced by the surface environment so as to lose their hysteretic behaviour, as already suggested by magneto-optical investigations.^[25]

Conclusions

In conclusion, the present investigation confirms that grafting large molecular clusters on conducting surfaces is not a straightforward process and is accompanied by significant modification in electronic and spin structures, which are not detected by standard surface characterization. In particular, although XPS and STM investigations suggest that intact Mn_{12} clusters are present as monolayers on the gold surface, the XAS reveals a systematic, partial reduction to Mn^{II} . The XMCD analysis suggests that these Mn^{II} ions are not present as isolated paramagnetic species and that the magnetic polarization at metal sites is decreased as compared with bulk complexes. Our results are therefore still compatible with the hypothesis that reduction of deposited clusters does not dramatically alter their chemical composition and size. A tendency of Mn_{12} clusters to undergo reduction at gold surfaces has indeed been recently predicted by density functional theory calculations.^[26] The observed XAS and XMCD spectra, however, indicate that the involved process is not a simple one-electron transfer from the substrate. Furthermore, the details of the reduction (average oxidation state and ratio of oxidation states) are very sensitive to the adopted deposition protocol. Finally, a deeper investigation of the best available sample failed to reveal any magnetic hysteresis. Though additional investigations are required to fully ascertain the structural and electronic features of Mn_{12} adsorbates on gold, the analysis reported herein demonstrates the potential of a combined use of XAS and XMCD to characterise magnetic molecular materials at surfaces. Studies can be carried out without significant sample damage, while retaining sufficient sensitivity to probe monolayers and even submonolayers of molecules. The possibility to work in high magnetic fields and at sub-Kelvin temperatures contributes to include the described approach and experimental setup into the available state-of-the-art investigation tools in molecular magnetism.

Experimental Section

Details concerning the experimental setup are presented in the Supporting Information. Spectra on powder samples have been obtained by pressing the freshly prepared crystalline material over a copper plate as sample holder. Ultra-thin film samples were freshly prepared under con-

trolled environment following preparation methods described elsewhere.^[11,12] STM imaging was carried out by using a NT-MDT Solver P47-Pro setup (NT-MDT, Zelenograd, Moscow, Russia; <http://www.ntmdt.ru/>) equipped with custom low-current pre-amplifier. All the STM measurements were carried out in constant current mode. Tips were prepared by mechanical sharpening of a Pt/Ir (90:10) wire; all measurements were carried out in air. Typical acquisition parameters used $U=1.8$ V, $I=4.5$ pA for monolayers of **2**, $U=0.4$ V, $I=15$ pA for submonolayers of **3** from tetrahydrofuran solutions and $U=0.8$ V, $I=6$ pA for monolayers of the same complex from dichloromethane solutions. The removal of the adsorbate in the upper part of Figure 4c was achieved by a previous scanning with $U=0.1$ V, $I=20$ pA. All the XAS spectra were acquired at BESSY II synchrotron in the UE46-PGM insertion device beamline by using the low temperature TBT XMCD set-up in the total electron yield detection mode. Special care was taken to minimise photoreduction effects (e.g. working at low photon flux). In the adopted conditions, the spectra showed no time dependence. The XMCD signal for a monolayer sample of **2** has been measured at $T=4.2$ K and in a magnetic induction of 2 T. The XMCD signal for **3** as a submonolayer deposit from THF and in the bulk phase has been measured at $T=4.2$ K and in a magnetic induction of 4 T. The XMCD signal for **3** as monolayer deposit from CH_2Cl_2 has been measured in a magnetic induction of 4 T at $T=0.5$ K by using the dilution setup described in ref. [27]. The analysis has been carried out taking into account these differences as reported in the Supporting Information. The analysis of the XAS and XMCD spectra has been performed by linear combination of experimental reference spectra with magnetic polarization parallel to the external magnetic field; we normalised the integrals of the reference signals following the sum rules for the number of holes as explained in ref. [28]; further details are provided in the Supporting Information; the reported percentage of oxidation states have an estimated error of $\pm 5\%$.

Acknowledgements

We gratefully acknowledge BESSY staff for helpful support, Dr. Paolo Imperia for assistance during XMCD measurements and Donella Rovai for the synthesis of the reduced Mn_{12} complex. We are glad to thank Jean-Paul Kappler for his instrumental support. We would like to thank Andrea Dei for the powerful discussions that enhanced the quality of this paper. This work was supported by the European Community—Research Infrastructure Action under the FP6 “Structuring the European Research Area” Programme (through the Integrated Infrastructure Initiative “Integrating Activity on Synchrotron and Free Electron Laser Science”—Contract R II 3-CT-2004-506008). The financial support was provided also by EC through NoE MAGMANet (NMP3-CT-2005-515767), QueMolNa (MRTN-CT-2003-504880), by Italian MIUR through FIRB (RBNE033KMA) and PRIN projects, and by Italian CNR (Commissa PM.P05.011).

- [1] D. Gatteschi, R. Sessoli, J. Villain, *Molecular Nanomagnets*, Oxford University Press, Oxford, **2006**.
- [2] a) J. M. Tour, M. Kozaki, J. M. Seminario, *J. Am. Chem. Soc.* **1998**, *120*, 8486; b) C. Romeike, M. R. Wegewijs, W. Hofstetter, H. Schoeller, *Phys. Rev. Lett.* **2006**, *97*, 206601; c) L. Bogani, W. Wernsdorfer, *Nat. Mater.* **2008**, *7*, 179.
- [3] a) M. R. Freeman, B. C. Choi, *Science* **2001**, *294*, 1484; b) A. Zhao, Q. Li, L. Chen, H. Xiang, W. Wang, S. Pan, B. Wang, X. Xiao, J. Yang, J. G. Hou, Q. Zhu, *Science* **2005**, *309*, 1542.
- [4] A. Nitzan, M. A. Ratner, *Science* **2003**, *300*, 1384.
- [5] a) H. B. Heersche, Z. de Groot, J. A. Folk, H. S. J. van der Zant, C. Romeike, M. R. Wegewijs, L. Zobbi, D. Barreca, E. Tondello, A. Cornia, *Phys. Rev. Lett.* **2006**, *96*, 206801; b) M.-H. Jo, J. E. Grose, K. Baheti, M. Deshmukh, J. J. Sokol, E. M. Rumberger, D. N. Hendrickson, J. R. Long, H. Park, D. C. Ralph, *Nano Lett.* **2006**, *6*, 2014.
- [6] R. Wiesendanger, H.-J. Güntherodt, G. Güntherodt, R. J. Gambino, R. Ruf, *Phys. Rev. Lett.* **1990**, *65*, 247.
- [7] a) Y. Manassen, R. J. Hamers, J. E. Demuth, A. J. Castellano, Jr., *Phys. Rev. Lett.* **1989**, *62*, 2531; b) P. Messina, M. Mannini, A. Caneschi, D. Gatteschi, L. Sorace, P. Sigalotti, C. Sandrin, S. Prato, P. Pittana, Y. Manassen, *J. Appl. Phys.* **2007**, *101*, 053916.
- [8] R. Sessoli, D. Gatteschi, A. Caneschi, M. A. Novak, *Nature* **1993**, *365*, 141.
- [9] a) J. R. Friedman, M. P. Sarachik, J. Tejada, R. Ziolo, *Phys. Rev. Lett.* **1996**, *76*, 3830; b) L. Thomas, F. Lionti, R. Ballou, D. Gatteschi, R. Sessoli, B. Barbara, *Nature* **1996**, *383*, 145.
- [10] a) A. Cornia, A. C. Fabretti, L. Zobbi, A. Caneschi, D. Gatteschi, M. Mannini, R. Sessoli in *Single-Molecule Magnets and Related Phenomena, Structure & Bonding*, Vol. 122 (Ed.: R. Winpenny), Springer, Heidelberg, **2006**, p. 133; b) S. Voss, M. Burgert, M. Fonin, U. Groth, U. Rüdiger, *Dalton Trans.* **2008**, 499.
- [11] A. Cornia, A. C. Fabretti, M. Pacchioni, L. Zobbi, D. Bonacchi, A. Caneschi, D. Gatteschi, R. Biagi, U. Del Pennino, V. De Renzi, L. Gurevich, H. S. J. Van der Zant, *Angew. Chem.* **2003**, *115*, 1683; *Angew. Chem. Int. Ed.* **2003**, *42*, 1645.
- [12] a) L. Zobbi, M. Mannini, M. Pacchioni, G. Chastanet, D. Bonacchi, C. Zanardi, R. Biagi, U. Del Pennino, D. Gatteschi, A. Cornia, R. Sessoli, *Chem. Commun.* **2005**, 1640; b) F. Pineider, M. Mannini, R. Sessoli, A. Caneschi, D. Barreca, L. Armelao, A. Cornia, E. Tondello, D. Gatteschi, *Langmuir* **2007**, *23*, 11836.
- [13] S. Voss, M. Fonin, U. Rüdiger, M. Burgert, U. Groth, Yu. S. Dedkov, *Phys. Rev. B* **2007**, *75*, 045102.
- [14] a) S. Voss, M. Fonin, U. Rüdiger, M. Burgert, U. Groth, *Appl. Phys. Lett.* **2007**, *90*, 133104; b) M. Burgert, S. Voss, S. Herr, M. Fonin, U. Groth, U. Rüdiger, *J. Am. Chem. Soc.* **2007**, *129*, 14362.
- [15] A. Naitabdi, J.-P. Bucher, Ph. Gerbier, P. Rabu, M. Drillon, *Adv. Mater.* **2005**, *17*, 1612.
- [16] a) R. V. Martínez, F. García, R. García, E. Coronado, A. Forment-Aliaga, F. M. Romero, S. Tatay, *Adv. Mater.* **2007**, *19*, 291.
- [17] U. del Pennino, V. De Renzi, R. Biagi, V. Corradini, L. Zobbi, A. Cornia, D. Gatteschi, F. Bondino, E. Magnano, M. Zangrando, M. Zacchigna, A. Lichtenstein, D. W. Boukhvalov, *Surf. Sci.* **2006**, *600*, 4185.
- [18] P. Gambardella, A. Dallmeyer, K. Maiti, M. C. Malagoli, W. Eberhardt, K. Kern, C. Carbone, *Nature* **2002**, *416*, 301.
- [19] H. Wende, M. Bernien, J. Luo, C. Sorg, N. Ponpandian, J. Kurde, J. Miguel, M. Piantek, X. Xu, Ph. Eckhold, W. Kuch, K. Baberschke, P. M. Panchmatia, B. Sanyal, P. M. Oppeneer, O. Eriksson, *Nat. Mater.* **2007**, *6*, 516.
- [20] P. Ghigna, A. Campana, A. Lascialfari, A. Caneschi, D. Gatteschi, A. Tagliaferri, F. Borgatti, *Phys. Rev. B* **2001**, *64*, 132413.
- [21] R. Moroni, Ch. Cartier dit Moulin, G. Champion, M.-A. Arrio, Ph. Sainctavit, M. Verdaguer, D. Gatteschi, *Phys. Rev. B* **2003**, *68*, 064407.
- [22] a) H. J. Eppley, H.-L. Tsai, N. de Vries, K. Folting, G. Christou, D. N. Hendrickson, *J. Am. Chem. Soc.* **1995**, *117*, 301; b) S. M. J. Aubin, Z. Sun, L. Pardi, J. Krzystek, K. Folting, L.-C. Brunel, A. L. Rheingold, G. Christou, D. N. Hendrickson, *Inorg. Chem.* **1999**, *38*, 5329.
- [23] M.-A. Arrio, A. Sculler, Ph. Sainctavit, Ch. Cartier dit Moulin, T. Mallah, M. Verdaguer, *J. Am. Chem. Soc.* **1999**, *121*, 6414.
- [24] M. Soler, S. K. Chandra, D. Ruiz, E. R. Davidson, D. N. Hendrickson, G. Christou, *Chem. Commun.* **2000**, 2417.
- [25] L. Bogani, L. Cavigli, M. Gurioli, R. L. Novak, M. Mannini, A. Caneschi, F. Pineider, R. Sessoli, M. Clemente-Leon, E. Coronado, *Adv. Mater.* **2007**, *19*, 3906.
- [26] S. Barraza-Lopez, M. C. Avery, K. Park, *Phys. Rev. B* **2007**, *76*, 224413.
- [27] I. Letard, Ph. Sainctavit, Ch. Cartier dit Moulin, J.-P. Kappler, P. Ghigna, D. Gatteschi, B. Doddi, *J. Appl. Phys.* **2007**, *101*, 113920.
- [28] B. T. Thole, G. van der Laan, M. Fabrizio, *Phys. Rev. B* **1994**, *50*, 11466.

Received: April 11, 2008
Published online: July 9, 2008